

# IMPRECISION IN GEODETIC OBSERVATIONS CASE STUDY GPS MONITORING NETWORKS

Steffen Schön and Hansjörg Kutterer

*Deutsches Geodätisches Forschungsinstitut (DGFI), Marstallplatz 8, D-80539 Munich, Germany*

## Abstract

The total error budget of geodetic observations is usually considered as being composed of exclusively random contributions (stochasticity). Typical measures for this type of uncertainty are confidence regions such as point confidence ellipsoids. However, this classical concept is incomplete as there is also uncertainty due to remaining systematics (imprecision) which is treated more adequately by real intervals. In this case interval boxes and convex polyhedra (zonotopes) are more meaningful uncertainty measures. Results for stochasticity and imprecision are exemplarily shown for GPS phase observations in case of monitoring networks.

## 1. Motivation

It is common practice to consider uncertainty in geodetic observations exclusively in terms of random effects (stochasticity). This strategy is easy to apply and it is conform with the recommendations of the Guide to the Expression of Uncertainty in Measurements (GUM), ISO (1995). However, the uncertainty of a corrected observation which results from preprocessing steps does not only contain a stochastic part but also remaining unknown systematic effects. Hence, besides stochasticity also *imprecision* has to be taken into account which is caused by imprecise or imperfect knowledge of external influences on the measurement procedure or by model simplifications. The term *imprecision* may not be common in geodesy, but as it is standard in the fuzzy logic or soft computing community (Kruse et al., 1994) it will be used in the following.

Fig. 1 gives a graphical motivation of the main idea of this paper. Assume that the standard deviation of one observation equals  $\sigma = 1$  and that an unknown systematic component remains whose possible magnitude is assessed with  $r = 0.3\sigma$ . If both components are treated as stochastic and hence combined using the variance propagation law, then the *combined uncertainty*  $u_c$  yields

$$u_c = \sqrt{\sigma^2 + r^2} = 1.04 \sigma . \quad (1)$$

If this observation is repeated  $n$  times,  $u_c$  can decrease beyond any limits, what does not correspond with practical experiences, (cf. the point-lined curve in Fig. (1)).

If only the stochastic part is treated by means of a variance and the remaining systematic part in a deterministic way, the two components of uncertainty are just added:

$$u_E = \sigma + r = 1.3 \sigma . \quad (2)$$

The resulting *extended uncertainty*  $u_E$  behaves as indicated by the black curve in Fig. 1, i.e. only the stochasticity is decreased by observation repetition but the imprecision remains unchanged. Obviously, such a characteristics meets reality better.

In a first part of this paper, the concept of interval analysis is briefly introduced and applied to describe imprecision. Using GPS phase measurements as an example, it is shown how interval radii can be derived as measures of imprecision. Finally, a simulated GPS monitoring network is analysed with respect to both parts of uncertainty. As a benefit of this new concept, a more realistic description of the uncertainty of the network point positions is obtained.

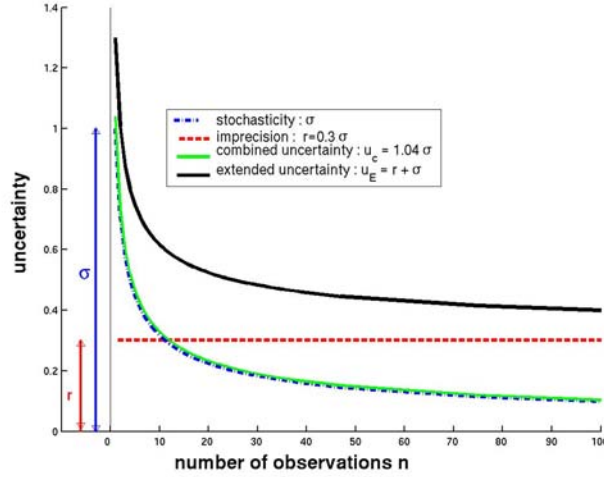


Figure 1: Extended and combined uncertainty

## 2. Elements of interval mathematics

In this section, some elements of interval mathematics are summarized which are necessary for the understanding of the paper. The basic reference is Alefeld and Herzberger (1983). A new textbook with applications to engineering sciences is Jaulin et al. (2001).

A real *interval*  $[a]$  is defined as a closed compact subset of the set of real numbers  $\mathfrak{R}$  and can be written as:

$$[a] = [a_l, a_u] = \{ t \in \mathfrak{R} \mid a_l \leq t \leq a_u, \quad a_l, a_u \in \mathfrak{R} \}, \quad (3)$$

where  $a_l$  denotes the lower and  $a_u$  the upper bound. Using the following transformation

$$a_m = \frac{a_u - a_l}{2}, \quad a_r = \frac{a_l + a_u}{2}, \quad (4)$$

an equivalent representation of the interval is given by its midpoint  $a_m$  and radius  $a_r$ :

$$[a] = \langle a_m, a_r \rangle, \quad a_m \in \mathfrak{R}, \quad a_r \in \mathfrak{R}_0^+. \quad (5)$$

The elementary *arithmetic operations* for intervals are defined as results of the application of the corresponding real operations to all elements of the intervals. Three main differences have to be noted in this context which are important for the developments explained in this paper. First, subtraction is not any longer inverse to addition because only the midpoints are subtracted but the radii are added

$$[a] - [b] = \langle a_m, a_r \rangle - \langle b_m, b_r \rangle \Rightarrow [a] - [a] = \langle a_m, a_r \rangle - \langle a_m, a_r \rangle = \langle 0, 2a_r \rangle. \quad (6)$$

Second, the law of distributivity is only valid in a generalized form (subdistributivity):

$$[a]([b] + [c]) \subseteq [a][b] + [a][c]. \quad (7)$$

Third, the multiplication of an interval  $[a]$  with a real scalar  $\gamma$  is given by:

$$\gamma [a] = \langle \gamma a_m, |\gamma| a_r \rangle. \quad (8)$$

The *interval extension of a real vector-valued function*  $f$  is defined by the substitution of the real vector  $\mathbf{x}$  by the interval vector  $[\mathbf{x}]$ :

$$f([\mathbf{x}]) := \{ f(\mathbf{x}) \mid \mathbf{x} \in [\mathbf{x}] \}. \quad (9)$$

Let  $f$  be a linear mapping expressed by the matrix  $\mathbf{D} = \mathbf{B} \mathbf{C}$ . Then the application of  $f$  to an interval vector  $[\mathbf{x}]$  leads to an interval vector:

$$[\mathbf{y}] = \mathbf{D} [\mathbf{x}] = \langle \mathbf{D} \mathbf{x}_m, |\mathbf{D}| \mathbf{x}_r \rangle \quad (10)$$

with the non-negative matrix  $|\mathbf{D}| = (|d_{ij}|) \geq \mathbf{0}$ . It is worth to mention, that the set of interval vectors is not closed with respect to mappings of type Eq. (9). In fact, the factual range of values is a central symmetrical convex polyhedron (*zonotope*, cf. Ziegler (1995, p. 198ff)):

$$Z := \{ \mathbf{y} \in \mathfrak{R}^m \mid \mathbf{y} = \mathbf{D} \mathbf{x}, \mathbf{x} \in [\mathbf{x}] \}. \quad (11)$$

However, the interval vector  $[\mathbf{y}]$  (Eq. (10)) represents an interval inclusion of the zonotope with respect to the chosen coordinate system.

$$Z \subseteq [\mathbf{y}] = (\mathbf{B C})[\mathbf{x}] \subseteq \mathbf{B}(\mathbf{C}[\mathbf{x}]). \quad (12)$$

Because of the subdistributivity, cf. Eq. (7), the smallest interval inclusion can be reached only if the real matrix multiplication is done before the multiplication with an interval vector, cf. Kutterer (1995).

### 3. Interval-based description of remaining systematics in GPS phase observations

In this section, intervals are used to describe remaining systematics. In a first part, the necessity of corrections on the original observations is motivated. In a second part, interval radii are used as corresponding non-stochastic measures of imprecision.

The geodetic model for the estimation of point positions is based on the Euclidean distance between the satellite  $S_k$  and the receiver  $P_i$ . Hence different corrections are necessary to take into account effects like tropospheric or ionospheric refraction, or eccentricities caused by instrumental heights as well as phase center variation or offsets, cf. Teunissen and Kleusberg (1998, p. 188ff).

The correction steps for GPS observations are rather sophisticated and depend mainly on the size and purpose of the network as well as on the intentions of the user. Therefore many different analysis strategies exist. Concerning the correction steps, some effects may be partially corrected for example, but also residual terms (like tropospheric delays) could be estimated as additional parameters during the adjustment. In addition, different differencing levels (zero, single, double, or triple differences) can be used in order to reduce or eliminate the impact of perturbing effects without modeling them explicitly. The following formula presents the basic relation for the carrier phase measurements (in [m]) between the station  $P_i$  and the satellite  $S_k$  at epoch  $t$  expressed in GPS time:

$$\begin{aligned} \Phi_i^k(t) = & \rho_i^k(t, t - \tau_i^k) - I_i^k + T_i^k + \delta m_i^k + c \left( dt_i(t) - dt^k(t - \tau_i^k) \right) + \\ & c \left( \delta_i(t) - \delta^k(t - \tau_i^k) \right) + \lambda \left( \phi_i(t_0) - \phi^k(t_0) \right) + \lambda N_i^k. \end{aligned} \quad (13)$$

The first part of Eq. (13) equals the Euclidian distance between the satellite and the receiver at epoch  $t$ , i.e. the basic geometric model. The travel time is given by  $\tau_i^k$ . Corrections  $I_i^k$ , and  $T_i^k$  are applied due to ionospheric and tropospheric refraction, respectively. The fourth part indicates the impact of signal multipath. The fifth part contains the clock errors terms, and the sixth part is introduced to handle delays in the measurement equipment. The last two terms result from non-zero initial phases and the carrier phase ambiguity, cf. Teunissen and Kleusberg (1998, p. 187ff). In general, a noise term  $\varepsilon_i^k(t)$  is associated with the phase measurement which describes the stochasticity of the observations.

Some systematic effects remain despite all correction steps during the data analysis. In general, they are due to only approximately or imprecisely known external influences or to model approximations. In the following an interval-based strategy is proposed to tackle these effects. First, all parameters  $\mathbf{p}$  (*influence parameters*) have to be identified which are imprecisely known and which have an impact on the corrected observations. These are, e.g., the coordinates of the satellite orbits  $\mathbf{x}^k$ , constants or parameters of correction models like the TEC value or the elevation angle of the satellite, or auxiliary measurements like meteorological parameters. Second, these parameters are expressed by intervals, i.e. the actual values of the parameters correspond to the interval midpoints and the imprecision to the radii. The magnitude of the imprecision can be derived from the temporal range of parameters or from the sensitivity of sensors used to determine the auxiliary measurements. In addition, model approximations or unmodeled effects are enclosed by intervals.

The main idea of the interval-based strategy is to ask for maximum impact of the influence parameter on the corrected observations (worst case). A straightforward approach is based on the *sensitivity analysis* of the correction models and analysis strategy. Using the total differential of Eq. (13) with respect to the influence parameters at a given epoch  $t$  yields:

$$d\Phi_i^k = d\rho_i^k(\mathbf{x}_i, \mathbf{x}^k) - dI_i^k(c_j, f, TEC, z_i^k, \dots) + dT_i^k(\vartheta_i, p_i, e_i, c_j, z_i^k, \dots) + \dots + \Delta_i^k. \quad (14)$$

For simplicity, only the first three terms are explicitly given. The first one denotes the total differential of the pseudo range depending on the orbit coordinates  $\mathbf{x}^k$ . The second term describes the impact of the ionospheric refraction model, which depends on influence parameters like e.g., some model constants  $c$ , the frequency  $f$ , the total electron content TEC, or the zenith angle of the satellite. The next one denotes the total differential of the tropospheric refraction model. These models are in general influenced by the meteorological parameters, like, e.g., temperature  $\vartheta_i$ , pressure  $p_i$ , or humidity  $e_i$ , model constants  $c_i$ , and the zenith angle  $z_i^k$  of the satellite. The other terms of Eq. (13) which are not given here can be differentiated in the same way. The last part  $\Delta_i^k$  assesses the impact of unmodeled effects and rounding-off errors.

Let  $\mathbf{f}_i^k$  denote the vector of partial derivatives and  $\mathbf{dp}$  the vector of differentials of the above-mentioned influence parameters. Then Eq. (14) can be rewritten as:

$$d\Phi_i^k = (\mathbf{f}_i^k)^T \mathbf{dp}. \quad (15)$$

Considering now the station  $P_i$  and the reference station  $P_j$ , the satellite  $S_k$  and the reference satellite  $S_l$ , then the double differences (DD) read as:

$$\Phi_{ij}^{kl} := \Phi_i^k - \Phi_j^k - \Phi_i^l + \Phi_j^l = \mathbf{M}\Phi. \quad (16)$$

Stacking all transposed vectors  $\mathbf{f}_i^k$  together in a matrix  $\mathbf{F}$  and applying Eq. (15) to Eq. (16), the differential of the DD is given by:

$$d\Phi_{ij}^{kl} := d\Phi_i^k - d\Phi_j^k - d\Phi_i^l + d\Phi_j^l = \mathbf{M}\mathbf{F}\mathbf{dp}. \quad (17)$$

In order to manage *worst-case behaviour*, the differentials  $\mathbf{dp}$  have to be interpreted as imprecision (interval radius) of the corresponding influence parameters. Eq. (18) gives the final results:

$$\Phi_{ij,m}^{kl} = \Phi_{ij}^{kl}, \quad \Phi_{ij,r}^{kl} = |\mathbf{M}\mathbf{F}|\mathbf{dp}, \quad (18)$$

The interval radius  $\Phi_{ij,r}^{kl}$  describes the imprecision of the corrected DD observations, whereas the interval midpoint  $\Phi_{ij,m}^{kl}$  is equal to the corrected DD observation  $\Phi_{ij}^{kl}$ .

Finally, the interval of the corrected observation which describes adequately its imprecision is reconstituted with the interval midpoint and radius:

$$\left[ \Phi_{ij}^{kl} \right] = \left[ \Phi_{ij,m}^{kl} - \Phi_{ij,r}^{kl}, \Phi_{ij,m}^{kl} + \Phi_{ij,r}^{kl} \right]. \quad (19)$$

This approach is very useful to analyse the contributions of special influence factors to the whole imprecision. Similar studies can be carried out for other types of observations like code measurements or the study of linear combinations. A more detailed example for EDM measurements is presented in Schön and Kutterer (2001).

#### 4. Interval extension of least-squares adjustments

In the previous section a mathematical tool was introduced to deal with remaining systematics in corrected DD GPS phase measurements. Now these effects are propagated to the estimated coordinates. For the sake of simplicity it is assumed that the ambiguities are resolved and no additional parameters like residual tropospheric delays are modeled. The following is based on Kutterer (1994) and Schön and Kutterer (2001) who proposed an *interval extension* of the least-squares estimator. The two different types of uncertainty (stochasticity and imprecision) are treated separately.

Let  $E(\mathbf{I})$  be the expectation of the vector of observations  $\mathbf{I}$ ,  $\mathbf{A}$  the  $n \times u$  configuration matrix, i.e. the matrix of the partial derivatives, and  $\mathbf{a}_0$  the zero-order vector of the Taylor expansion. Then a linearized Gauss-Markov model, cf. Koch (1999), is given by:

$$\begin{aligned} E(\mathbf{I}) &= \mathbf{A}\mathbf{dx} + \mathbf{a}_0 \\ D(\mathbf{I}) &= \sigma_0^2 \mathbf{P}^{-1} \end{aligned} \quad (20)$$

The stochastic model is given by the dispersion matrix  $D(\mathbf{I})$  of the observations, where  $\mathbf{P}$  denotes their weight matrix and  $\sigma_0^2$  the a-priori variance factor. Assuming uncorrelated initial zero differenced (ZD), i.e. original, phase measurements, the dispersion matrix of the DDs becomes

$$D(\mathbf{I}) = \mathbf{M}\mathbf{M}^T,$$

where  $\mathbf{M}$  indicates the matrix of the differencing method, cf. Eq. (16). A datum constraint (no net translation) is added in order to solve the adjustment problem:

$$\mathbf{d}\hat{\mathbf{x}} = \mathbf{Q}_{\hat{\mathbf{x}}} \mathbf{A}^T \mathbf{P} (\mathbf{l} - \mathbf{a}_0), \quad \mathbf{Q}_{\hat{\mathbf{x}}} = (\mathbf{A}^T \mathbf{P} \mathbf{A})^{-1}. \quad (21)$$

An interval extension of Eq. (21), i.e. replacing the vector of the corrected observations  $\mathbf{l}$  by determined interval vector  $[\mathbf{l}]$ , cf. Eq. (9):

$$[\mathbf{d}\hat{\mathbf{x}}] = \mathbf{Q}_{\hat{\mathbf{x}}} \mathbf{A}^T \mathbf{P} ([\mathbf{l}] - \mathbf{a}_0). \quad (22)$$

According to Eq. (4), Eq. (22) can be split into a midpoint and a radius part. The zero-order vector  $\mathbf{a}_0$  is considered as point interval vector, i.e.  $\mathbf{a}_{0,m} = \mathbf{a}_0$ ,  $\mathbf{a}_{0,r} = \mathbf{0}$ .

$$\begin{aligned} \mathbf{d}\hat{\mathbf{x}}_m &= \mathbf{Q}_{\hat{\mathbf{x}}} \mathbf{A}^T \mathbf{P} (\mathbf{l}_m - \mathbf{a}_0), \\ \mathbf{d}\hat{\mathbf{x}}_r &= \left| \mathbf{Q}_{\hat{\mathbf{x}}} \mathbf{A}^T \mathbf{P} \right| \mathbf{l}_r. \end{aligned} \quad (23)$$

The midpoint  $\mathbf{l}_m$  is the actual value for the corrected observation vector  $\mathbf{l}$ . Eq. (23a) is identical with the classical least-squares estimate, which takes into account the stochastic information about the observations contained in the dispersion matrix  $D(\mathbf{l})$ . The imprecision modeled by the interval approach is *linearly* propagated to the estimates, cf. Eq. (23b). As we have seen in Section 1, Eq. (22) is the tightest enclosure of the zonotope which expresses the imprecision of the point position:

$$Z = \left\{ \mathbf{d}\hat{\mathbf{x}} \in \mathfrak{R}^n \mid \mathbf{d}\hat{\mathbf{x}} = (\mathbf{Q}_{\hat{\mathbf{x}}} \mathbf{A}^T \mathbf{P}) (\mathbf{l} - \mathbf{a}_0), \mathbf{l} \in [\mathbf{l}] \right\}. \quad (24)$$

## 5. Example: GPS Monitoring Network

Using the example of a simulated GPS network, we show in this section the behaviour of both components of uncertainty, stochasticity and imprecision.

Fig. (2) shows the sky distribution of the satellites during one hour of observation time. The local network consists of nine points located approximately  $49^\circ$  N Lat. and  $9^\circ$  E Long.. Choosing the central point as reference point, eight baselines can be selected with baseline lengths of 1 km and 1.4 km. Hence, the shape of the network can be considered as typical for local networks like monitoring networks. The standard deviation of the ZDs is  $\sigma = 2 \text{ mm}$ , the interval radius describing the is  $r = 0.5 \text{ mm}$ . The ambiguities are assumed as resolved, and standard correction models are applied.

A double difference approach which is standard in GPS analysis software like the Bernese Software (Hugentobler et al., 2001) is used to reduce or eliminate the impact of the major effects, discussed in Section 3. Due to the small network extension, similar (meteorological) conditions can be assumed for the different stations. Hence for this homogeneous situation, the impact of ionospheric or tropospheric refraction is cancelled when using DDs. For an processing interval of  $t_I = 1200 \text{ sec}$ ,  $n_I = 224$  DDs can be computed, using a cut-off angle of  $10^\circ$ .

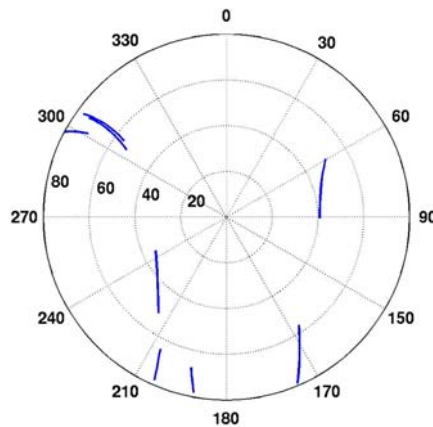


**Figure 2:** Satellite sky distribution

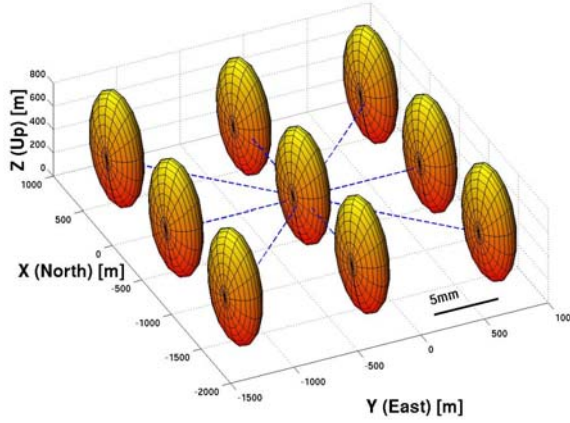


Figure 3a: 3d 95% confidence ellipsoids

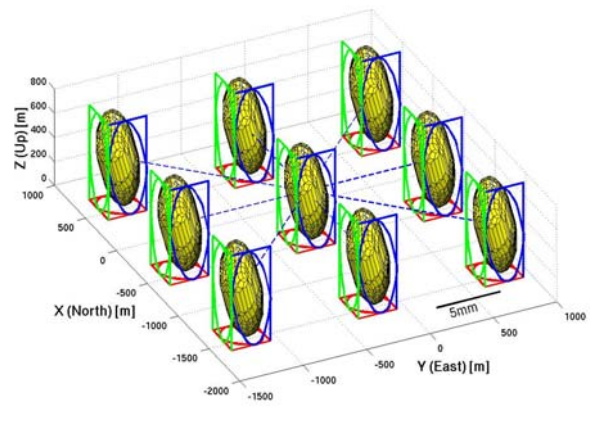


Figure 3b: 3d zonotopes

Fig. (3a) shows the 95% confidence ellipsoids of the estimated point position for the above described simulation scenario I. The 95% confidence ellipsoids are given in a unique local topocentric coordinate system for all stations. The lengths of the semi-axes are  $a=5.4\text{ mm}$ ,  $b=2.1\text{ mm}$ , and  $c=1.3\text{ mm}$ . The standard deviations of the coordinates are equal for all points:  $\sigma_N=0.4\text{ mm}$ ,  $\sigma_E=0.5\text{ mm}$ , and  $\sigma_{Up}=3.8\text{ mm}$ . The semimajor axis of the 95% confidence ellipsoids is oriented to the South-East ( $Az=58.5^\circ$ ,  $El=81.6^\circ$ ), what is due to the specific satellite distribution depicted in Fig. (2) which shows some gaps in the North-South direction.

Fig. (3b) presents the corresponding three-dimensional zonotopes (grey-shaped) which describe the imprecision of the estimated point positions due to remaining systematics. In addition, the interval boxes which enclose the zonotopes are plotted. Zonotopes and interval boxes are computed with respect to Eqs. (23) and (24). The interval radii of the coordinates are  $x_r=1.6\text{ mm}$ ,  $y_r=1.5\text{ mm}$ , and  $z_r=3.9\text{ mm}$ . The orientation of the zonotopes is similar to those of the confidence ellipsoids which is due to the geometry of the scenario contained in the configuration matrix  $\mathbf{A}$ . For both point uncertainty measures (confidence ellipsoids and zonotopes), the concrete shape is equal for all points of the network. Hence, the choice of the reference point and reference satellite does not have any impact on the uncertainty of the estimated point positions.

Now, we will show how an increase of the number of observations influences the above presented uncertainty measures of the estimated point positions. Therefore a second scenario II is simulated by choosing a processing rate of  $t_2 = 360\text{sec}$  for the same observation time of 1h. On the one hand, this choice guarantees the same geometrical situation of the adjustment problem as in scenario I. On the other hand it assures an increase of the number of observations to  $n_2 = 595$  double differences. In order to compare and easily discuss the different results, two-dimensional projections of the three-dimensional 95% confidence ellipsoids and zonotopes are considered.

Fig. (4a) gives a representation of the projected three dimensional confidence ellipsoids for both scenarios: In grey the initial scenario with  $n_1 = 224$  observations and in black the second scenario with  $n_2 = 595$  observations is shown. For both scenarios, all confidence ellipsoids have the same shape and orientation. Due to the quadratic variance-covariance propagation which is intrinsic to the classical stochastic approach, all confidence ellipsoids of scenario II lie inside those of scenario I. The standard deviation yields  $\sigma_N=0.2\text{ mm}$ ,  $\sigma_E=0.2\text{ mm}$ , and  $\sigma_{Up}=1.5\text{ mm}$ , which corresponds to a mean reduction of 60%.

Fig (4b) shows a graphic comparison of the projected zonotopes. For these convex polytopes a totally different behavior is shown. In grey the results of scenario I are plotted, in black (dotted line) those corresponding to scenario II. Contrary to the confidence ellipsoids, the zonotopes of scenario II have approximately the same size as those of scenario I or even enclose the latter ones:  $x_r=1.6\text{ mm}$ ,  $y_r=1.6\text{ mm}$ ,  $z_r=4.2\text{ mm}$ .

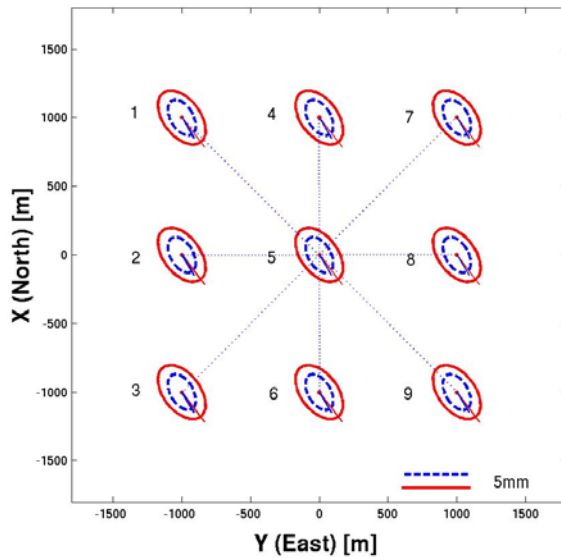


Figure 4a: Comparison of the 95% confidence ellipsoids

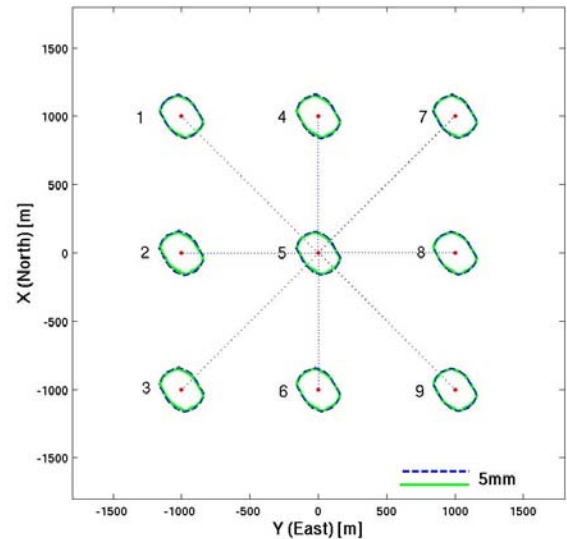


Figure 4b: Comparison of zonotopes

To understand the underlying mechanisms we have to look closer at Eq. (24). Two main mechanisms play a key role for the linear propagation of the imprecision. On the one hand, a plus of (more or less redundant) observations strengthens the geometry of the adjustment problem. As a result, a more favorable propagation could be expected like for the variances. But on the other hand, a plus of observations increases the whole imprecision, i.e. the total amount of systematics we have to consider. These two antipodal effects play the key role for the understanding of the imprecision propagation. In this application the influence of both mechanisms is balanced what can be expressed by the fact that the resulting interval radii increase only by maximum 5 % for the height component. Schön and Kutterer (2001) obtained similar results for a two-dimensional network. They showed that an improvement of the network geometry can decrease the imprecision to a certain amount. Contrary, the addition of only redundant observations – as it is the case here – can not reduce the imprecision.

## 6. Conclusions

In this paper an extended approach was presented for the treatment of the two most relevant types of uncertainty, namely stochasticity and imprecision. Imprecision can be seen as a second type of uncertainty due to remaining systematics. In many geodetic applications both types have to be taken into account. Hence, the classical stochastic description of uncertainty has to be extended. The effects of imprecision are adequately treated by interval mathematics provided that meaningful observation intervals are available. In Section 3 a method was outlined to solve this task in geodetic practice. The imprecision of the observations is propagated to the estimated parameters using the interval extension of the least-squares estimator.

In a last section the application of the new concept to a GPS network was shown. In case of GPS measurements there are many redundant observations. An exclusively stochastic assessment of uncertainty yields standard deviations of the estimated parameters which can decrease beyond any limit what contradicts the experience of surveying practitioners. One step further is the superposition of the measures for stochasticity and imprecision which were treated in this study side by side. A concrete solution for such a superposition based on the theory of fuzzy sets was developed by Kutterer (2002).

## Acknowledgements

The presented paper shows results and new ideas developed during the research project KU 1250 /1-1 and KU 1250 1/2 “Optimaler Entwurf geodätischer Überwachungsnetze unter Berücksichtigung strenger Toleranzen”, which is sponsored by the Deutsche Forschungsgemeinschaft (DFG). This is gratefully acknowledged by the authors. Thanks to Klaus Kanuith and Manuela Krügel (both at DGFI) for helpful advises on the Bernese Software.

## References

- Alefeld G. and J. Herzberger (1983). *Introduction to Interval Computations*. Academic Press, New York, 333p.
- ISO (1995): *Guide to the Expression of Uncertainty in Measurements*. German translation: Leitfaden zur Angabe der Unsicherheit beim Messen. Deutsches Institut für Normung, Beuth Verlag, Berlin.
- Hugentobler U., S. Schaer and P. Fridez (2001). *Bernese GPS Software Version 4.2*, Astronomical Institute University of Berne.
- Jaulin L., Kieffer M., Didrit O. and Walter E. (2001). *Applied Interval Analysis*, Springer, London, 379p.
- Koch K.-R. (1999). *Parameter Estimation and Hypothesis Testing in Linear Models* (2<sup>nd</sup> Ed.). Springer, Berlin.
- Kruse R., Gebhardt J., Klawonn F. (1994). *Foundations of Fuzzy Systems*. Wiley, Chichester, UK.
- Kutterer H. (1994). *Intervallmathematische Behandlung endlicher Unschärfen linearer Ausgleichungsmodelle*, DGK C 423, München.
- Kutterer H. (1995). The effect of fuzzy weight matrices on the results of least squares adjustments, In: F. Sans\_ (Ed.): *Geodetic Theory Today. IAG Symposium* No. 114, Springer, Berlin, 224-234.
- Kutterer H. (2002). Joint treatment of random variability and imprecision in GPS data analysis. *Journal of Global Positioning Systems*, 1(2), 96-105.
- Schön S. and Kutterer H. (2001). Optimal Design of geodetic Monitoring networks by means of interval mathematics. In: C. Whitacker (Ed.): *Proceedings of the 10<sup>th</sup> FIG International Symposium on Deformation Analysis*, Orange California, 41-46.
- Teunissen P. and A. Kleusberg (1998). GPS observation equation and positioning concepts. In: Teunissen P and A. Kleusberg (Eds): *GPS for Geodesy* (2<sup>nd</sup> Ed), Springer, Berlin , 187-230.
- Ziegler G. M. (1995): *Lectures on Polytopes*. Springer, New York.